









Study on the Influence of Aspect Ratio of Photovoltaic Panel Models on Wind Tunnel Pressure Test Results

Mao Yan¹, Bin Zhang^{2*}, Xinling Fan², Shidong Nie¹, Min Liu¹ and Huaizhong Huang¹

¹ School of civil engineering, Chongqing University, Chongqing 400045, PR China

² PowerChina Guiyang Engineering Corporation Limited, Guiyang. 550081, PR China
zhangbin_gyy@powerchina.cn

Abstract. Currently, wind tunnel pressure tests are commonly used to study the wind load characteristics of photovoltaic structures, by reducing the aspect ratio of the photovoltaic panels to meet the testing requirements. This study investigates the influence of model width/thickness ratio on the wind pressure resistance test results of rigid models of photovoltaic panels. The results indicate that the smaller the width-to-thickness ratio, the greater the impact on the test results, with the leeward side having a greater influence than the windward side. The influence of the model width/thickness ratio on the test results decreases with increasing tilt angle of the photovoltaic panel. The width and thickness ratio of the model have a significant impact on the measured wind pressure values, but a minor impact on wind pressure variations.

Keywords: Wind tunnel test; Photovoltaic panels; Scale model; Aspect ratio.

1 Introduction

Photovoltaic pressure testing is a commonly used measurement method ^[1]. Ma et al. conducted studies on the inclination effect and interference effect of PV modules ^[2]. In wind tunnel experiments, Alrawashdeh et al. ^[3] found through wind tunnel tests that the model scale ratio significantly affects the wind load on photovoltaic panels at certain wind angles, but has little impact at the most adverse wind angle. Aly ^[4] studied the scale ratio of models and found that it has minimal impact on the average wind load on photovoltaic panels, but significant impact on extreme wind loads. This impact can be mitigated by adjusting the turbulence of the wind field and improving the test setup.

Furthermore, other researchers have found that when air passes through a rectangular section, flow separation occurs around the rectangular section, followed by vortex shedding ^[5-9], with significant differences in this process for rectangular sections of different aspect ratios. From the above studies, it can be inferred that the flow field characteristics and wind load properties on the surface of photovoltaic panel models may also be influenced by the aspect ratio of the models. This study

investigates the influence of the width-to-thickness ratio of PV scale models on wind tunnel pressure test results.

2 Experimental Overview

2.1 Experimental Wind Field and Model Description

Experimental Wind Field. The experiment was conducted in the DC wind tunnel laboratory at Chongqing University. This experiment was carried out in a low turbulence empty-field (5.77%) and a high turbulence grille field (14.82%) (Fig. 1).

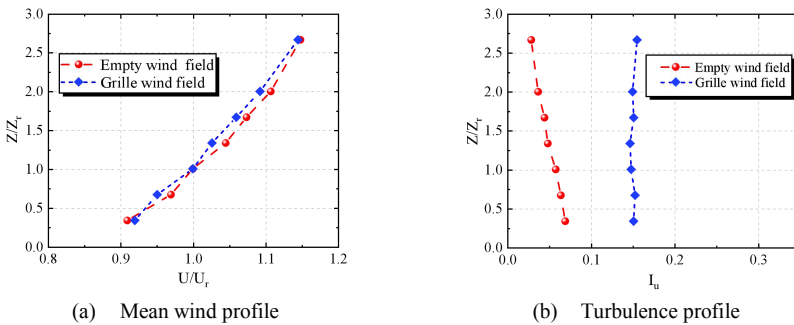


Fig. 1 Test results of wind field

Model Conditions. The experiment selected a single photovoltaic structure composed of 6 photovoltaic modules, which was fabricated into a segmented model (Fig. 2).



Fig. 2. Wind tunnel pressure test model diagram.

Table 1. Model number and test parameters.

Model number	Model size	Width-to-thickness ratio	Measuring point arrangement	Number of points
TC-02a	322mm×91mm×2mm	41.5	Upper surface	18
TC-02b	322mm×91mm×2mm	41.5	Lower surface	18
TC-08	322mm×91mm×8mm	11.4	two-sided	36
TC-10	322mm×91mm×10mm	9.1	two-sided	36
TC-12	322mm×91mm×12mm	7.6	two-sided	36

Test Condition. The geometric scaling ratio, time scaling ratio and wind speed scaling ratio are 1:25, 1:10 and 1:2.5 respectively for the wind tunnel pressure test of the rigid model of photovoltaic panels. The wind direction angles of the test were 0° and 180° , and the inclination angles of the photovoltaic panel were 15° , 30° and 60° (Fig. 3).

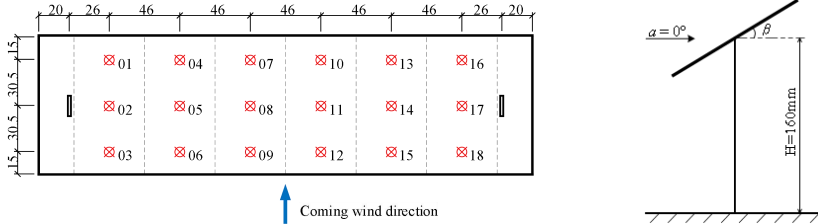


Fig. 3. Model measuring point layout diagram and Model diagram.

2.2 Data Processing and Analysis

The wind pressure coefficient is defined as the ratio of the pressure caused by the incoming wind on the surface of the photovoltaic panel to the reference velocity pressure measured at the reference height position, and the instantaneous wind pressure coefficient of each measurement point is expressed as:

$$C_{Pi} = \frac{P_i(t) - P_\infty}{P_0 - P_\infty} \quad (1)$$

The calculation formula of average wind pressure coefficient and pulsating wind pressure coefficient is as follows:

$$C_{Pi,mean} = \frac{1}{N} \sum_{t=1}^N C_{Pi}(t) \quad (2)$$

$$C_{Pi,rms} = \sqrt{\frac{1}{N-1} \sum_{t=1}^N [C_{Pi}(t) - C_{Pi,mean}]^2} \quad (3)$$

In formula (2) and (3), $C_{Pi,mean}$ and $C_{Pi,rms}$ are respectively the average and pulsating wind pressure coefficients of the measuring point i . N is the total number of wind pressure data collection at the measuring point.

3 Test results and analysis

3.1 Average wind pressure coefficient

The results in Fig. 4 indicate that reducing the width-to-thickness ratio of the models led to significant differences in the net mean wind pressure coefficients measured for the three models compared to the standard scale model under the 0° inclination condition. As the inclination angle increased, the net mean wind pressure coefficients for all models increased, and the difference between the thickened model and the standard scale model decreased. The smaller the width/thickness ratio of the

photovoltaic panel model, the greater the difference. When the slope was 15° and 30°, the measured net mean wind pressure coefficients of the models decreased with decreasing width-to-thickness ratio compared to those of the standard scale model. When the slope was 60°, the net mean wind pressure coefficients measured for the models were slightly larger than the standard scale model but very close, as the width-to-thickness ratio decreased.

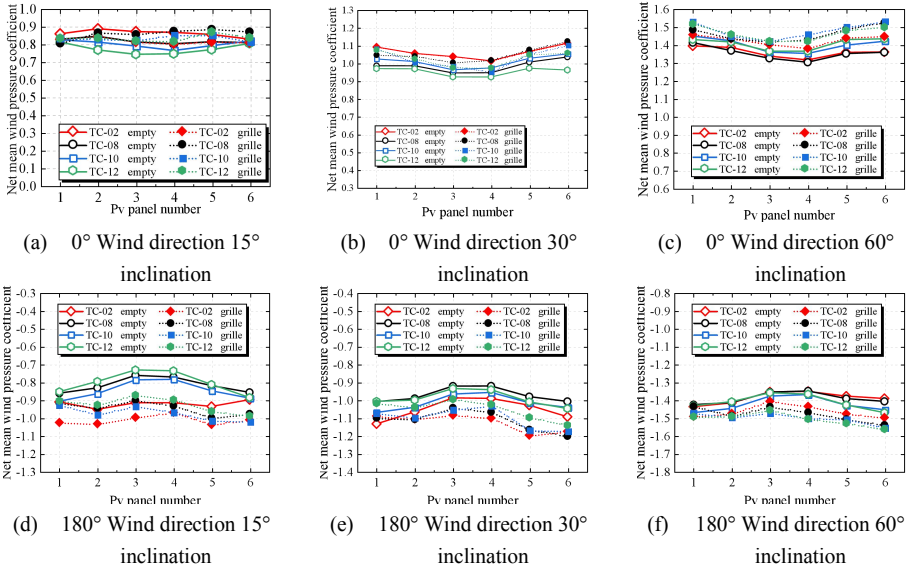


Fig. 4. The net average wind pressure coefficient of the model.

3.2 Fluctuating wind pressure coefficient

From the results in Figures 5 and 6, it can be observed that in the high turbulence grid field, the surface fluctuating wind pressure coefficients measured for the same model are higher than those in the empty-field. When the inclination angle is 0°, the upper surface fluctuating wind pressure coefficients of the thickened model under both wind field conditions are greater than those of the standard scale model, and the difference is significant. When the wind direction is 0° and the inclination angles are 15°, 30°, and 60°, the lee surface fluctuating wind pressure coefficients of the thickened models are similar to those of the standard scale model, but slightly higher, indicating that as the width-to-thickness ratio decreases, the difference becomes larger. For the same model, as the inclination angle increases, the fluctuating wind pressure coefficients on the upper surface also increase.

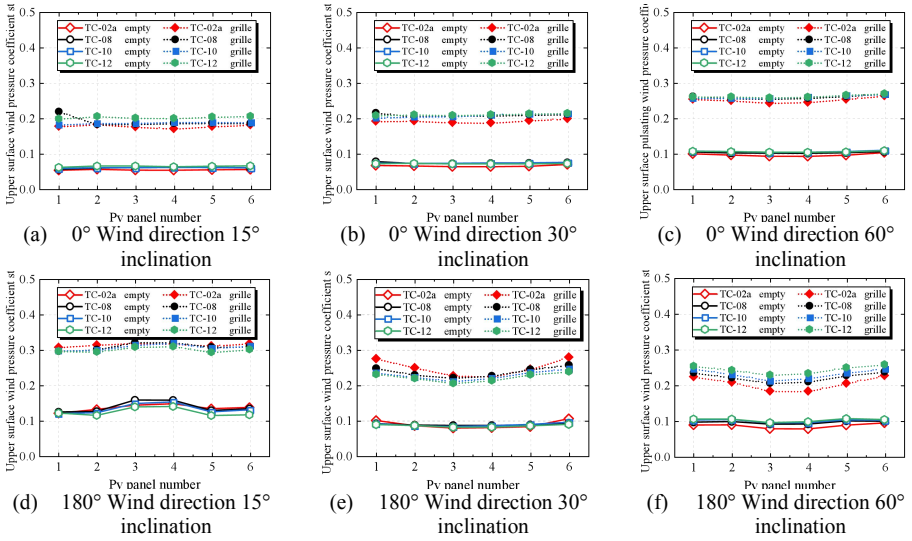
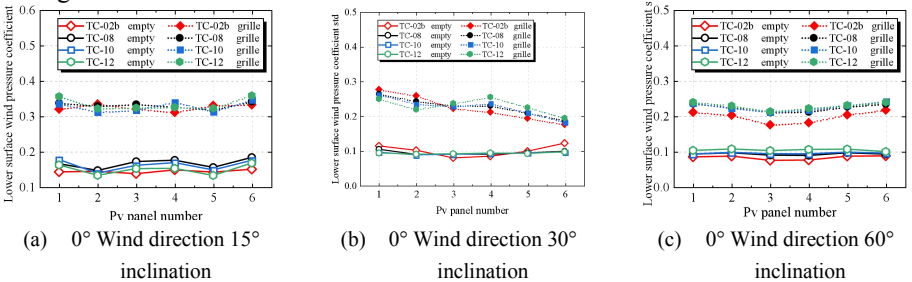


Fig. 5. The fluctuating wind pressure coefficient of the upper surface of the Pv panel.

When the wind direction angle is 180° and the inclination angle is 15°, the fluctuating wind pressure coefficients on both sides of the upper surface (leeward side) of the photovoltaic panel model in the open wind field are relatively high. The difference in the fluctuating wind pressure coefficients on the upper surface of the thickened model compared to the standard scale model is noticeable, while the difference between the fluctuating wind pressure coefficients on the upper surface of the thickened model and the standard scale model is not as pronounced. At an inclination angle of 30°, the fluctuating wind pressure coefficients on the upper surface of the thickened model in the open wind field are slightly lower on the sides and slightly higher in the center compared to the standard scale model. In the grid field, the overall fluctuating wind pressure coefficients on the upper surface are higher on the sides than in the center, and the fluctuating wind pressure coefficients on the upper surface of the thickened model are lower than those of the standard scale model. Under a 60° inclination angle, the fluctuating wind pressure coefficients on the upper surface of the thickened model are higher than those of the standard scale model.



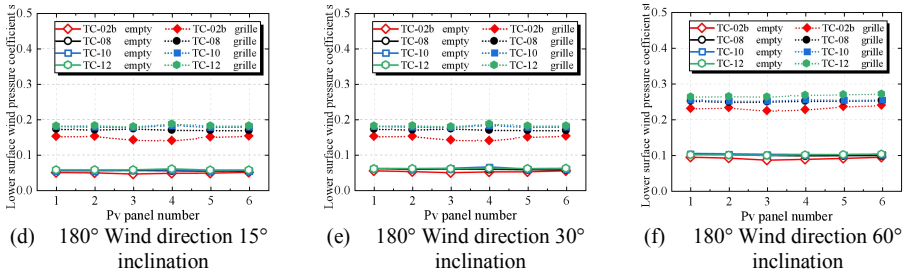


Fig. 6. The fluctuating wind pressure coefficient of the lower surface of the Pv panel.

3.3 Extreme Wind Pressure Coefficient

In this paper, the extreme wind pressure coefficients at measurement points are calculated using the PHPM model with no feasible zone constraints proposed by Liu et al.^[10] through the definition of new statistical moments. From Figure 7, it can be seen that under the 0° inclination condition, the extreme wind pressure coefficients on the upper surface measured for various thickened models in two wind fields differ significantly from the standard scaled model; at wind directions of 0° and 180°, when the inclination angles are 15°, 30°, and 60°, the extreme wind pressure coefficients on the upper surface measured for various thickened models in the open field are similar to those of the standard scaled model, while in the grid field, the differences are greater, and the smaller the aspect ratio, the greater the difference; due to the higher turbulence in the grid field, the extreme wind pressure coefficients measured for the same model in the grid field are significantly greater than those measured in the open field.

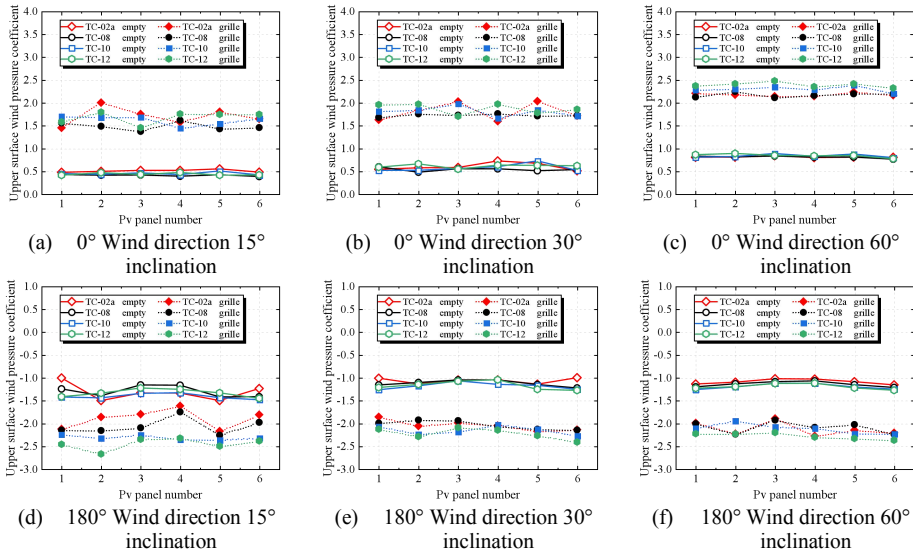


Fig. 7. The extreme wind pressure coefficient of the upper surface of the Pv panel.

From Figure 8, it can be seen that under the 0° and 15° inclination conditions, the extreme wind pressure coefficients on the lower surface measured for various thickened models in two wind fields show significant differences compared to the standard scaled model; at inclination angles of 30° and 60°, the extreme wind pressure coefficients on the lower surface measured for various thickened models in the open field are very similar to those of the standard scaled model, while in the grid field, the differences are slightly larger, and follow the pattern that the smaller the aspect ratio, the greater the difference; due to higher turbulence in the grid field, the extreme wind pressure coefficients measured for the same model in the grid field are also significantly greater than those measured in the open field.

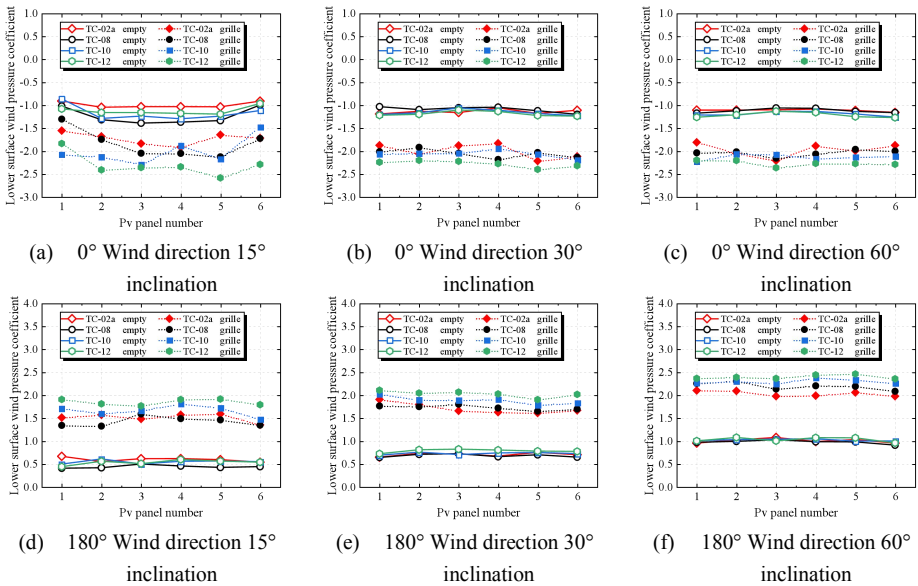


Fig. 8. The extreme wind pressure coefficient of the lower surface of the Pv panel.

4 Conclusion

In the wind tunnel pressure test of rigid models of photovoltaic structures, the smaller the width-to-thickness ratio of the photovoltaic panel model, the greater its impact on the test results. The specific conclusions are as follows:

- 1) As the inclination angle of the photovoltaic panel increases, the influence of the width-to-thickness ratio on the test results decreases.
- 2) For the fluctuating wind pressure coefficient and extreme wind pressure coefficient, the impact of the width-to-thickness ratio on the test results of the windward side of the photovoltaic panel is smaller than that on the leeward side, and the influence of the width-to-thickness ratio on both parameters increases with the increase in wind field turbulence.

3) The width-to-thickness ratio has a significant impact on the measured wind pressure values, but a relatively small impact on the wind pressure variation pattern.

References

1. Yang Q S , Shan W S , Tamura Y.: Characteristics of fluctuating wind loads on high-rise buildings. *China Civil Engineering Journal* , 56(05) (2023).
2. Ma W Y , Ma C C , Wang C Y , et al.: Wind tunnel experimental study on the wind load interference effect of photovoltaic arrays. *Experimental Fluid Mechanics*, 35(04) (2021).
3. Alrawashdeh H , Stathopoulos T.: Wind loads on solar panels mounted on flat roofs: Effect of geometric scale. *Journal of Wind Engineering & Industrial Aerodynamics* , 206 (2020).
4. Aly M A , Bitsuamlak G.: Aerodynamics of ground-mounted solar panels: Test model scale effects. *Journal of Wind Engineering & Industrial Aerodynamics* 123, 250–260 (2013).
5. Liu Y, Ke F, Sung H.: Unsteady separated and reattaching turbulent flow over a two-dimensional square rib. *Journal of Fluids and Structures* 24(3), 366–381 (2007).
6. Bearman P.W.: Some measurements of the distortion of turbulence approaching a two-dimensional bluff body. *Journal of Fluid Mechanics* 53(3), 451–467 (1972).
7. Bearman P.W.: An investigation of the forces on flat plates normal to a turbulent flow. *Journal of Fluid Mechanics* 46(1), 177–198 (1971).
8. Aditi S, Paul T.: Effects of forced frequency oscillations and free stream turbulence on the separation-induced transition in pressure gradient dominated flows. *Physics of Fluids*, 32(10), 1–21 (2020).
9. Nakamura Y.: The effects of turbulence on a separated and reattaching flow. *Journal of Fluid Mechanics* 178 477–490 (1987).
10. Liu M, Chen X, Yang Q.: Estimation of Peak Factor of Non-Gaussian Wind Pressures by Improved Moment-Based Hermite Model. *Journal of Engineering Mechanics*, 143(7), (2017).

Open Access This chapter is licensed under the terms of the Creative Commons Attribution-NonCommercial 4.0 International License (<http://creativecommons.org/licenses/by-nc/4.0/>), which permits any noncommercial use, sharing, adaptation, distribution and reproduction in any medium or format, as long as you give appropriate credit to the original author(s) and the source, provide a link to the Creative Commons license and indicate if changes were made.

The images or other third party material in this chapter are included in the chapter's Creative Commons license, unless indicated otherwise in a credit line to the material. If material is not included in the chapter's Creative Commons license and your intended use is not permitted by statutory regulation or exceeds the permitted use, you will need to obtain permission directly from the copyright holder.

